



PERGAMON

Micron 34 (2003) 319–325

**micron**

[www.elsevier.com/locate/micron](http://www.elsevier.com/locate/micron)

## Sidelobe decline in single-photon 4Pi microscopy by Toraldo rings

M. Martínez-Corral<sup>a,\*</sup>, M.T. Caballero<sup>b</sup>, A. Pons<sup>a</sup>, P. Andrés<sup>a</sup>

<sup>a</sup>*Departamento de Óptica, Universidad de Valencia, 46100 Burjassot, Spain*

<sup>b</sup>*Departamento de Óptica, Universidad de Alicante, 03080 Alicante, Spain*

### Abstract

We demonstrate theoretically the feasibility of single-photon 4Pi-confocal microscopy. By inserting a pair of properly designed multi-ring phase-only pupil filters in the illumination path of a 4Pi microscope the height of the sidelobes of the point spread function substantially reduced, so that there is no ambiguity in the 3D image. Then, an axial resolution up to four times higher than that of single-photon confocal microscope can be effectively achieved.

© 2003 Elsevier Ltd. All rights reserved.

*Keywords:* 4Pi microscopy; 3 Apodization; Toraldo filters

### 1. Introduction

Confocal scanning microscopy is an imaging technique whose main feature is its optical sectioning capacity (Wilson, 1990). The confocal technique was specifically designed to improve the axial resolution. However, it is notable that, due to the laws of diffraction, the resolution in the direction of the optical axis is, depending on the numerical aperture (NA) of the lenses, about three times poorer than its lateral counterpart (Pawley, 1995). This difference between axial and lateral resolution leads to anisotropic images of three-dimensional (3D) specimens.

One attempt to reduce this anisotropy is to insert in the illumination arm of the confocal setup a pupil filter composed by two equal-area transparent rings (Martínez-Corral et al., 1995). With this technique it is possible reduce the axial extent of the point spread function (PSF) up to a factor 1.5. A very ingenious, and efficient, technique for reducing the axial extent of the PSF is to create a standing wave by the interference of two opposing wave-fronts, as made in the so-called standing-wave microscopy (Bailey et al., 1993) and in 4Pi-confocal microscopy (Hell and Stelzer, 1992a). Standing-wave microscopy is a nonconfocal imaging technique, and therefore it does not provide any improvement in optical sectioning. In the 4Pi(c)-confocal microscope two opposing high-NA objectives are used for

coherently illuminating and detecting the same point of a fluorescent specimen. The resulting PSF has an axial main peak that is about four times narrower than its confocal counterpart. However, the narrowing of the main peak is accompanied by a severe enlargement of the secondary axial sidelobes, which lead to ambiguity in the image.

To overcome this problem, the use of two-photon excitation was proposed (Hell and Stelzer, 1992b; Nagorni and Hell, 2001a). Due to the squared dependence of the excitation on the illumination intensity, and the mismatch between the illumination and the fluorescence wavelength, the height of the secondary axial lobes is significantly reduced. Once the sidelobes have been reduced (which implies that the deep gaps in the optical transfer function (OTF) have been filled), data deconvolution techniques can be used to improve the quality of the image (Nagorni and Hell, 2001b).

What we report here is that by using a pair properly designed phase-only pupil filters, the axial sidelobes of the PSF can be strongly reduced. This implies that single-photon 4Pi-confocal microscopy can produce unambiguous 3D images, and thus makes it not necessary to resort to multi-photon processes. The phase-filters are designed according to the axial form of the Toraldo's pupil-synthesis method (Toraldo di Francia, 1952; Martínez-Corral et al., 2002a), and are composed of seven annular transparent zones. Each pair of neighboring zones have opposite phases. We will show, by means of a numerical experiment, that sidelobe height can be down to 7% of the main peak (compared to 23% without filters). In other words, the axial-

\* Corresponding author. Tel.: +34-96-386-4343; fax: +34-96-386-4715.  
E-mail address: [manuel.martinez@uv.es](mailto:manuel.martinez@uv.es) (M. Martínez-Corral).

OTF gaps are filled so that data deconvolution can be further applied.

## 2. The axial PSF

Consider a 4Pi(c)-confocal scanning microscope like the one schematically plotted in Fig. 1. In this kind of system the 3D specimen is illuminated by the standing wave generated by the interference between the two opposing, tightly focused waves proceeding from the high NA objectives. The light emitted by the fluorescent specimen is collected by the same objectives, and interfere at the pinhole plane. If we consider that the illuminating beam is linearly polarized, the 3D PSF of this imaging system is given by (Hell and Stelzer, 1992b)

$$I_{4\text{Pi}}(z, r, \varphi) = I_{\text{ill}}(r, z, \varphi)I_{\text{det}}(r, z) \\ = |\mathbf{E}(r, z, \varphi) + \mathbf{E}(r, -z, -\varphi)|^{2m} |\mathbf{E}(\varepsilon r, \varepsilon z) \\ + \mathbf{E}(\varepsilon r, -\varepsilon z)|^2, \quad (1)$$

where  $r$  and  $z$  are radial and axial coordinates, as measured from the focus of the wave-fronts. Random polarization of fluorescent light has been assumed. The parameter  $m$  defines the mode of excitation, e.g.  $m = 1$  denotes single-photon absorption, whereas  $\varepsilon = \lambda_{\text{exc}}/\lambda_{\text{det}}$  represents the ratio between the excitation and the fluorescence wavelength.

In Eq. (1) the function  $\mathbf{E}(r, z, \varphi)$  denotes the electric field in the focal region of an aberration-free lens illuminated by a linearly polarized plane wavefront. According to Richards and Wolf (1959)

$$\mathbf{E}(r, z, \varphi) = [I_0(r, z) + I_2(r, z)\cos 2\varphi]\mathbf{i} + I_2(r, z)\sin 2\varphi\mathbf{j} \\ - 2iI_1(r, z)\cos \varphi\mathbf{k}, \quad (2)$$

where  $I_{0,1,2}$  are integrals over the aperture angle  $\theta$ , and  $\varphi$  stands for the angle between the polarization direction of the incident field and the observation meridian plane.

To analyze the behavior of a 4Pi(c)-confocal microscope, we firstly center our attention in the axial component of the 3D PSF, which is governed by the function

$$E(r = 0, z) = I_0(r = 0, z) \\ = \int_0^\alpha A(\theta)(1 + \cos \theta)\exp\left(i2\pi n \frac{\cos \theta}{\lambda} z\right) \sin \theta d\theta. \quad (3)$$

In Eq. (3), which does not depend on the polarization direction  $\varphi$ ,  $n$  is the refractive index of the medium,  $\alpha$  is the semiaperture angle of the lens, and  $A(\theta)$  represents the apodization function, i.e. the amplitude transmittance of the aperture stop of the lens. This function depends on the angle  $\theta$ , to which the geometrical rays correspond to as seen from the nominal focal point. Next, it is convenient to

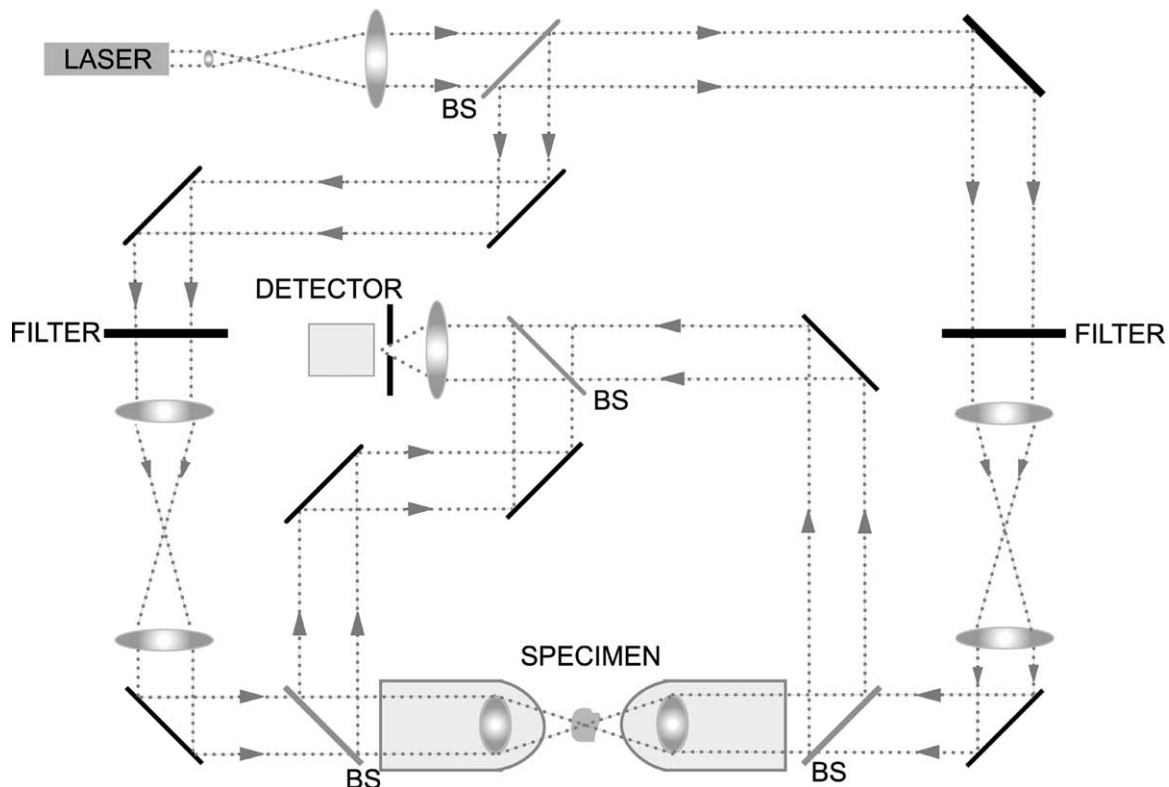


Fig. 1. Schematic geometry of a 4Pi(c) apodized confocal microscope. Relay lenses are used to focus the pupil filters into the back focal plane of the objective.

perform the nonlinear mapping

$$\zeta = \frac{\cos \theta - \cos \alpha}{1 - \cos \alpha} - 0.5; \quad Q(\zeta) = (1 + \cos \theta)A(\theta). \quad (4)$$

Eq. (3) can be then rewritten as

$$E(r=0, z) = (1 - \cos \alpha) \exp\left(i\pi n \frac{1 + \cos \alpha}{\lambda} z\right) \times \int_{-0.5}^{0.5} Q(\zeta) \exp\left(i2\pi n \frac{1 - \cos \alpha}{\lambda} z \zeta\right) d\zeta. \quad (5)$$

Now, according to Eqs. (1) and (5) the illumination and the detection axial PSFs can be expressed as

$$I_{\text{ill}}(r=0, z) = \left| 2(1 - \cos \alpha) \cos\left(\pi n \frac{1 + \cos \alpha}{\lambda_{\text{exc}}} z\right) \tilde{Q}(sz) \right|^{2m}, \quad (6)$$

and

$$I_{\text{det}}(r=0, z) = \left| 2(1 - \cos \alpha) \cos\left(\pi n \frac{1 + \cos \alpha}{\lambda_{\text{exc}}} \varepsilon z\right) \tilde{Q}(s\varepsilon z) \right|^2. \quad (7)$$

In the above equations  $\tilde{Q}$  represents the 1D Fourier transform of function  $Q$ , and  $s = n(1 - \cos \alpha) / \lambda_{\text{exc}}$  a scale

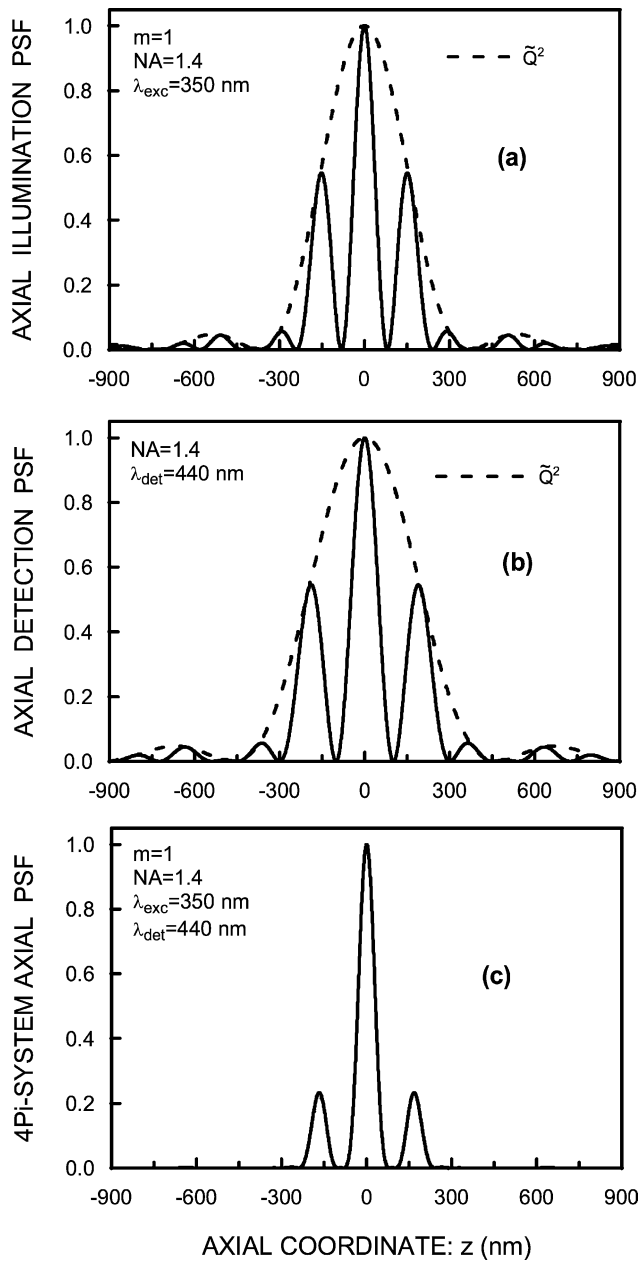


Fig. 2. Numerically evaluated axial intensity PSF corresponding to: (a) illumination system in case of single-photon absorption; (b) detection system (dashed curves correspond to the enveloping function); and (c) single-photon 4Pi(c)-confocal microscope.

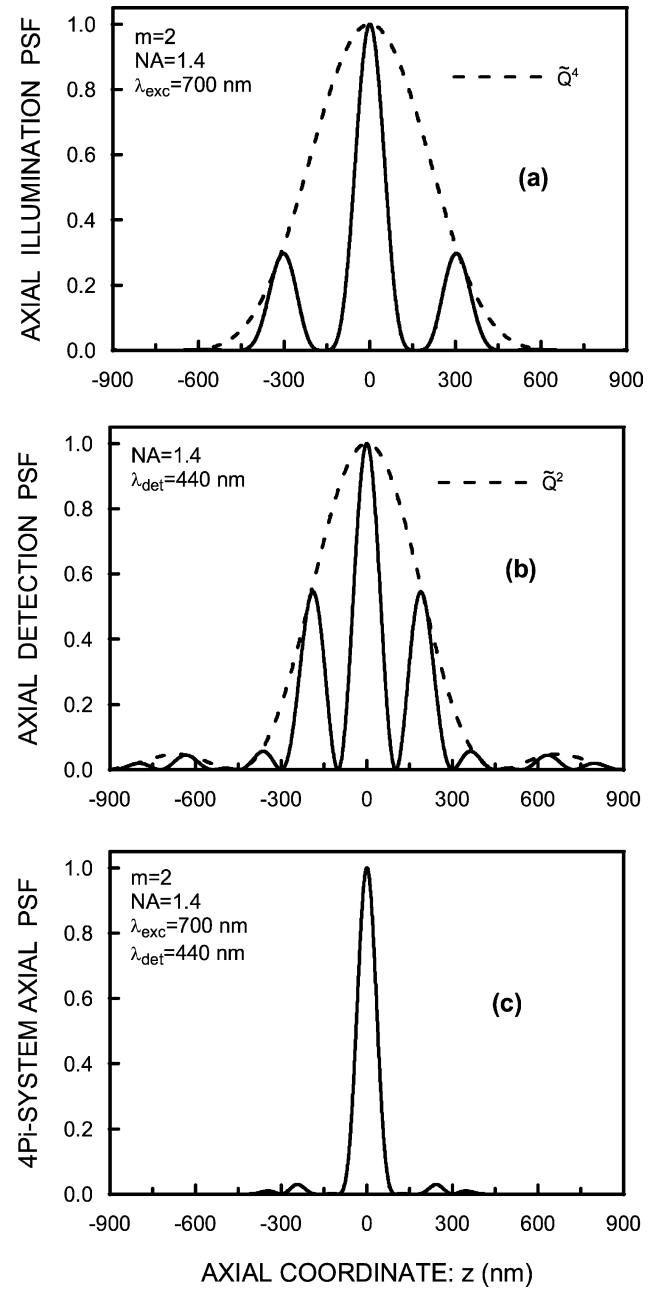


Fig. 3. Numerically evaluated axial intensity PSF corresponding to: (a) illumination system in case of two-photon absorption; (b) detection system (dashed curves correspond to the enveloping function); (c) two-photon 4Pi(c)-confocal microscope.

factor that depends on the parameters of the system. Note that the only differences between illumination and detection PSF are a power factor  $m$  and a scale factor  $1/\varepsilon$ .

In the particular case of single-photon absorption,  $m = 1$ , and clear circular apertures as the lenses' stops, the illumination axial PSF is given by the product between a  $\cos^2$  factor (the interference factor), whose period is proportional to  $\lambda_{\text{exc}}/(1 + \cos \alpha)$ , and a  $\tilde{Q}^2$  factor (the modulating factor), which closely approximates to  $\sin^2(s z)$ , and whose width is proportional to  $\lambda_{\text{exc}}/(1 - \cos \alpha)$ . Since the variation of the  $\tilde{Q}^2$  factor is in general much smoother than the one of the  $\cos^2$  factor, the variation of the illumination PSF can be seen as a  $\cos^2$  modulated by function  $\tilde{Q}^2$ . To obtain an illumination PSF with low sidelobes it is necessary that the width of the two factors be comparable and then that the ratio  $(1 + \cos \alpha)/(1 - \cos \alpha)$  be as low as possible. Therefore, if one wants to implement a 4Pi(c) microscope in which the axial sidelobes of the PSF be small, the NA of the objectives must be as high as possible.

An example of axial PSF is shown in Fig. 2, where we selected for the calculations the highest allowable NA. Then, in our numerical example we set  $n = 1.518$ ,  $\alpha = 67.5$  (NA = 1.4),  $\lambda_{\text{exc}} = 350$  nm and  $\varepsilon = 0.8$ . Note from this figure that illumination (Fig. 2a) and detection (Fig. 2b) axial PSFs exhibit a very narrow central lobe, but high axial sidelobes. The 4Pi-system PSF is obtained by multiplying the curves in Fig. 2a and b. The resulting curve has a central lobe whose width is imposed by the one of the illumination-PSF core. Due to the multiplicative process the height of the sidelobes has been down to 23% of the main peak. However, the sidelobes are still too high and they can produce artifacts in the 3D image.

To overcome the sidelobes problem, the use of two-photon absorption ( $m = 2$ ) was classically proposed (Hell and Stelzer, 1992b). In such case, the contribution of the secondary maxima of the illumination PSF is substantially reduced due to the squared dependence of the excitation on the illumination intensity (Fig. 3a). However, it should be noted here that the ability of two-photon excitation as a sidelobe-reducer tool in 4Pi-confocal microscopy mainly proceeds from the considerable difference between the excitation and the fluorescent wavelengths. An example of

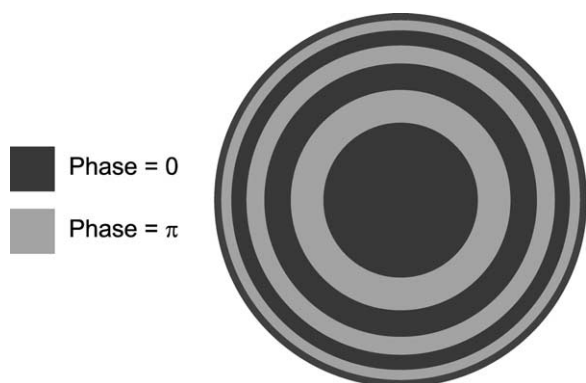


Fig. 4. Two-dimensional representation of the seven-zone Toraldo filter.

this is shown in Fig. 3 where we calculated the axial PSFs for the same NA as in Fig. 2, but with  $\lambda_{\text{exc}} = 700$  nm and  $\varepsilon = 1.6$ . Due to the wavelengths mismatch, the illumination and the detection PSFs have now quite different scales so that the secondary peak of the illumination PSF is multiplied by low value of the detection PSF. Additionally, the secondary peaks of the detection PSF are multiplied by low values of the illumination PSF. The multiplicative process yields to a significant reduction of the axial sidelobes of the 4Pi-system PSF. Note, however, that now the width of the central lobe is imposed by the collection

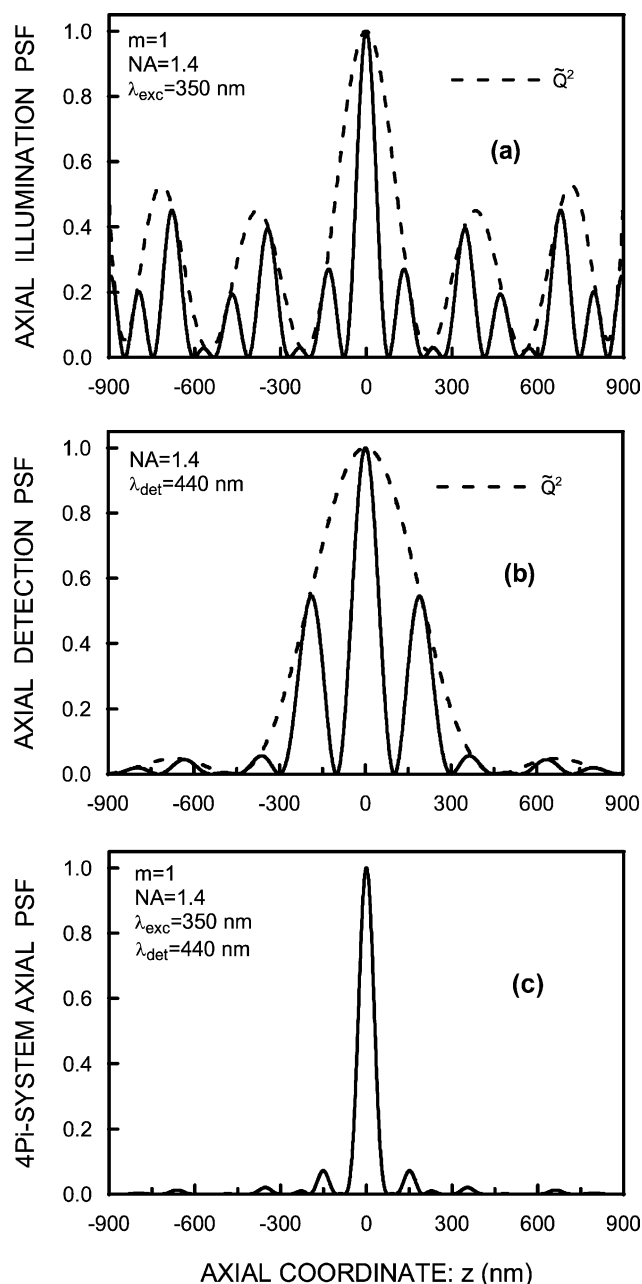


Fig. 5. Numerically evaluated axial intensity PSF corresponding to: (a) illumination system assuming single-photon absorption and that Toraldo filters are inserted; (b) detection system; and (c) single-photon 4Pi(c)-confocal microscope.

Table 1  
List of PSF figures corresponding to single-photon 4Pi, two-photon 4Pi, and single-photon 4Pi but with the Toraldo filters

	Axial intensity PSF		
	Main peak width at $I_{4\text{Pi}}(z) = 0.01$	Main peak width at $I_{4\text{Pi}}(z) = 0.5$ (FWHM)	Sidelobe relative height
Single photon 4Pi(c)	138 nm (100%)	63 nm (100%)	0.23 (100%)
Two photon 4Pi(c)	175 nm (127%)	76 nm (121%)	0.03 (13%)
Single photon 4Pi(c) with Toraldo filters	133 nm (96%)	61 nm (97%)	0.07 (30%)

wavelength and therefore is about 21% wider than the one obtained with single-photon absorption.

### 3. The use of Toraldo filters

In this paper we propose an alternative technique for reduction of axial sidelobes. As we show below, by placing in the illumination path of a single-photon 4Pi-confocal microscope, a pair of properly designed phase-only pupil filters it is possible to produce a significant reduction of the axial-PSF sidelobes, and therefore to make unnecessary the use of two-photon processes. The filters are inserted in the illumination path to avoid waste of fluorescence light.

What we need are pupil filters that permit to control the form of function  $\tilde{Q}$  so that the secondary peak of the illumination PSF is multiplied by low values of the detection PSF, and vice versa. In previous publications it has been proposed the use of dark ring (DR) filters to reach this goal (Blanca et al., 2001; Martínez-Corral et al., 2002b). However, the use of DR filters has two drawbacks: an important lost of light in the illumination process, and the existence of huge sidelobes in the illumination PSF, which could result in severe photo-bleaching of the specimen at the position of the strong secondary peak. We propose here the use of phase-only filters designed according to the axial

form of the Toraldo's pupil-synthesis method. By this method, which has been described elsewhere (Martínez-Corral et al., 2002a), one can design a pupil filter that controls the position of the zeros of the function  $\tilde{Q}$ .

Following the Toraldo's method we have designed a pupil filter that consists of seven annular zones. As shown in Fig. 4 the zones have no absorption, having each pair of neighboring zones opposite phases. The normalized radii for the zones are  $r_1 = 0.41$ ,  $r_2 = 0.56$ ,  $r_3 = 0.73$ ,  $r_4 = 0.83$ ,  $r_5 = 0.91$ ,  $r_6 = 0.96$  and  $r_7 = 1$ . Since the zones have no absorption the filter throughput is optimized. On the other hand, the choice of phase-only filters with constant transmittance in the annular zones yields to a design that can be manufactured with relative ease.

To show the power of our proposal we performed a numerical experiment in which we inserted two copies of the above filter in the illumination path of a single-photon 4Pi(c)-confocal microscope. The parameters for the calculation were the same as the ones used in Fig. 2. In Fig. 5 we have plotted the illumination and the detection PSFs, together with the PSF of the 4Pi system. Note that the use of the Toraldo filters in single-photon 4Pi microscopy produce an effect that is similar to the one produced by two-photon absorption, that is, the secondary maxima of the illumination PSF are multiplied by low values of the detection PSF and vice-versa. Importantly, the lobes are downed to 7% of the main peak, which is 3.3 times lower than the lobe height obtained without the Toraldo filter, and only slightly higher than the one obtained with two-photon excitation (Table 1). Other important figure, which is also listed in Table 1, is the width of the main peak. If we compare the techniques in terms of this parameter, which is closely related with the axial resolution, as defined in terms of Rayleigh criterion, we find that the apodized 4Pi setup is slightly better than the nonapodized, and importantly better ( $\sim 25\%$  improvement) than the two-photon mode.

Next, in Fig. 6 we compare, in contour plots, the 3D intensity distribution in the meridian plane  $\varphi = \pi/2$ ,

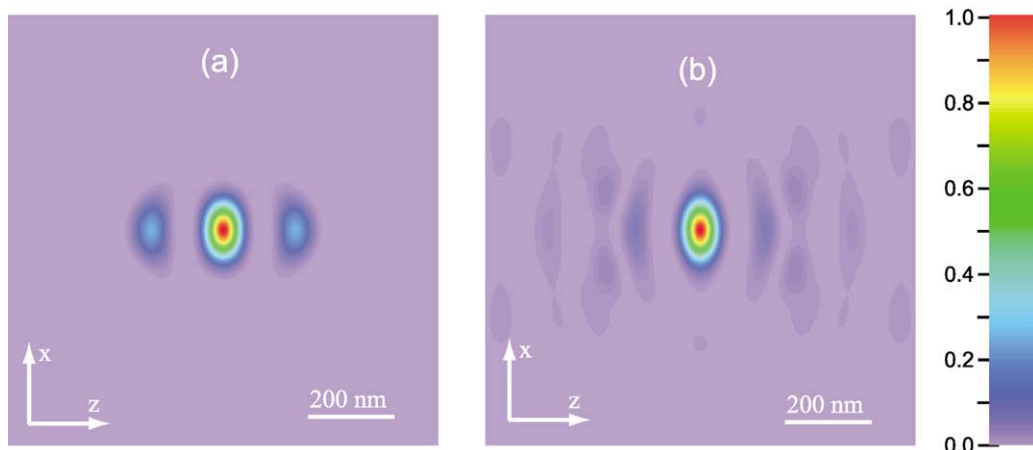


Fig. 6. Contour plot of the 3D intensity PSF in the meridian plane  $\varphi = \pi/2$  corresponding to: (a) 4Pi(c) single-photon confocal microscope; and (b) same as (a) but with the Toraldo filters inserted in the illumination path.

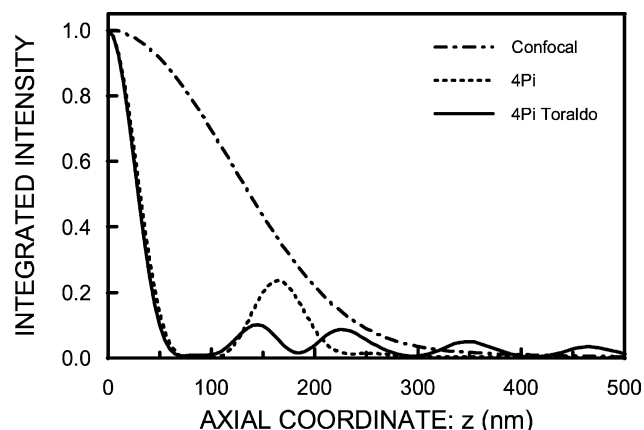


Fig. 7. Normalized  $z$ -response to an infinitely thin fluorescent layer.

corresponding to the single-photon 4Pi(c)-confocal microscope with and without the Toraldo filters. Note that, apart from strongly reducing the axial sidelobes, the use of Toraldo filters hardly affects the transverse resolution (0.04% wider at FWHM).

To complete the study the influence of the proposed technique on the performance of 4Pi-confocal microscope, in Fig. 7 we have plotted the integrated intensity (i.e. the  $z$  response to an infinitely fluorescent layer). Note that, as summarized in Table 2, the central lobe has been slightly

Table 2

List of integrated intensity figures corresponding to single-photon 4Pi, single-photon 4Pi, but with the Toraldo filters, and single-photon confocal scanning microscope

	Integrated intensity	
	Main peak width at $I_{\text{int}}(z) = 0.5$ (FWHM)	Sidelobe relative height
Single-photon 4Pi(c)	66 nm (100%)	0.25 (100%)
Single-photon 4Pi(c) with Toraldo filters	64 nm (97%)	0.10 (40%)
Single-photon confocal microscope	274 nm (415%)	–

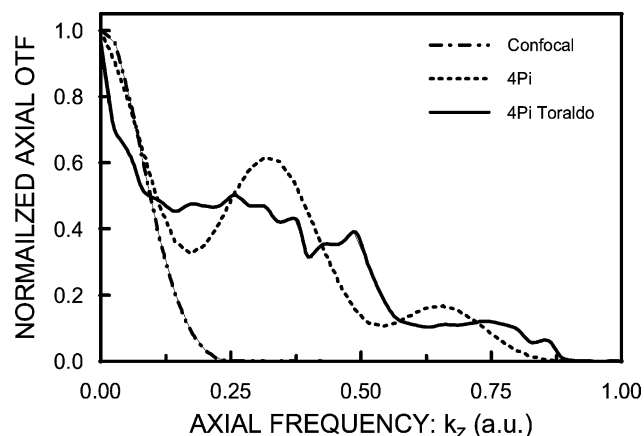


Fig. 8. Axial optical transfer function for the same cases as in Fig. 7.

narrowed and the maximum sidelobe height has been reduced from 0.25 to 0.10. Finally, in Fig. 8 we compare the OTF along the optical axis. The use of 4Pi geometry enlarges the axial bandwidth and the insertion of the Toraldo filters in the illumination path permits to fill the axial gaps of the OTF.

#### 4. Conclusions

We have demonstrated theoretically the viability of single-photon 4Pi-confocal microscopy. We show that by using multi-ring phase-only pupil filters in the illumination path of the microscope it is possible to down the axial sidelobes height to 7% of the main peak. This allows the system to receive the full benefit in axial resolution from a main peak that is about four times sharper than that of confocal microscope. Of course, the proposed system enhances the photo-bleaching as compared with the standard single-photon 4Pi microscope. But standard 4Pi single-photon microscopes do not produce useful images due to the strong sidelobes. The use of pupil filters in imaging systems always implies a trade-of. The main advantage of Toraldo filters, as compared with other pupil filters—as for example the DR filters—is that they produce the same reduction of the PSF sidelobes, but with smaller overall bleaching effect. The combination of the proposed technique with deconvolution techniques would make it unnecessary the use of multi-photon processes.

#### Acknowledgements

This work was supported the Plan Nacional I + D + I (Grant DPI2000-0774), Ministerio de Ciencia y Tecnología, Spain.

#### References

- Bailey, B., Farkas, D.L., Lansing-Taylor, D., Lanni, F., 1993. Enhancement resolution in fluorescence microscopy by standing-wave excitation. *Science* 366, 44–48.
- Blanca, C.M., Bewersdorf, J., Hell, S.W., 2001. Single sharp spot in fluorescence microscopy of two opposing lenses. *Appl. Phys. Lett.* 79, 2321–2323.
- Hell, S., Stelzer, E.H.K., 1992a. Properties of a 4Pi confocal fluorescence microscope. *J. Opt. Soc. Am. A* 9, 2159–2166.
- Hell, S., Stelzer, E.H.K., 1992b. Fundamental improvement of resolution with a 4Pi-confocal fluorescence microscope using two-photon excitation. *Opt. Commun.* 93, 277–282.
- Martínez-Corral, M., Andrés, P., Ojeda-Castañeda, J., Saavedra, G., 1995. Tunable axial superresolution by annular binary filters. Application to confocal microscopy. *Opt. Commun.* 119, 491–498.
- Martínez-Corral, M., Caballero, M.T., Stelzer, E.H.K., Swoger, J., 2002a. Tailoring the axial shape of the point spread function using the Toraldo concept. *Opt. Express* 10, 98–103.

- Martínez-Corral, M., Caballero, M.T., Pons, A., 2002b. Axial apodization in 4Pi-confocal microscopy by annular binary filters. *J. Opt. Soc. Am. A* 19, 1532–1536.
- Nagorni, M., Hell, S., 2001a. Coherent use of opposing lenses for axial resolution increase in fluorescence microscopy I. Comparative study of concepts. *J. Opt. Soc. Am. A* 18, 36–48.
- Nagorni, M., Hell, S.W., 2001b. Coherent use of opposing lenses for axial resolution increase. II. Power and limitation of nonlinear image restoration. *J. Opt. Soc. Am. A* 18, 49–54.
- Pawley, J. (Ed.), 1995. *Handbook of Biological Confocal Microscopy*, Plenum Press, New York.
- Richards, B., Wolf, E., 1959. Electromagnetic diffraction in optical systems. II. Structure of the image field in an aplanatic system. *Proc. Roy. Soc. (Lond), A* 253, 358–379.
- Toraldo di Francia, G., 1952. Nuovo pupille superresolventi. *Atti Fond. Giorgio Ronchi* 7, 366–372.
- Wilson, T. (Ed.), 1990. *Confocal Microscopy*, Academic Press, London.